Efficiency Estimation of Liquid–Liquid Hydrocyclones Using Trajectory Analysis

D. Wolbert, B.-F. Ma, and Y. Aurelle
Laboratoire de Traitements Physico-chimiques des Eaux, Département de Génie des Procédés Industriels, Institut National des Sciences Appliquées de Toulouse, Complexe Scientifique de Rangueil, F-31 077 Toulouse Cedex, France

J. Seureau
Elf Aquitaine Production, Département Environnement, Centre de Recherche de Boussens, F-31 360 Saint-Martory, France

As the use of hydrocyclones for liquid–liquid separation becomes increasingly common, the need for a satisfactory method to assess their efficiency increases. Currently available efficiency theories were developed for liquid–solid separations, based on the velocity distributions inside a hydrocyclone. These theories, however, appear less suitable for emulsions where the dispersed phase is slightly lighter than the continuous phase, such as oil/water emulsions. An efficiency computation based on the analysis of the trajectories of the droplets is presented. Trajectories are characterized through a differential equation combining models for the three bulk velocity distributions (axial, radial, and tangential) and the settling velocity defined by Stokes' law. From the critical trajectory and given operating conditions, a characteristic droplet diameter d_{100} can be deduced that corresponds to the smallest droplet with a 100% efficiency. Other efficiencies are obtained by changing the initial condition for the trajectory equation. The efficiency results of different hydrocyclone configurations are compared with experimental results, and residual emulsion distributions are estimated.

Introduction

Liquid–liquid mixtures, especially oil/water emulsions, are often encountered in the chemical and petrochemical industries. Their separation has been the subject of many studies in various fields. After simple decantation, several processes have been considered, such as flotation, coalescence, centrifugation, and cycloning.

The idea for hydrocyclones for solid–liquid separation came from the gas–solid cyclone used for dust collection. The energy of the fluid is used to generate a vortex effect. The vortex induces a centrifugal acceleration hundreds of times greater than the gravitational acceleration. The dispersed particles, subject to this force, will move either toward the wall, if their specific gravity is higher than the specific gravity of the continuous phase, or toward the core of the hydrocyclone otherwise.

Well suited to the separation of particles in the 10–300 μm range, several aspects of hydrocyclones make them particularly interesting:

- The maintenance requirements remain low due to the absence of moving parts.
- Setting up and operation are easy.
- Little space is required.
- Unlike other separators, their efficiency increases with flow rate.

Two hydrocyclone designs have been suggested for liquid–liquid separation. Rietema (1969) developed a hydrocyclone closely related to the conventional cyclones: a three-cell flow pattern is produced where the continuous phase leaves the apparatus through the overflow, while the concentrated oil emulsion is removed at the underflow outlet, the diameter of which has been reduced to the size of the oil core. Another design was developed by Colman and Thew

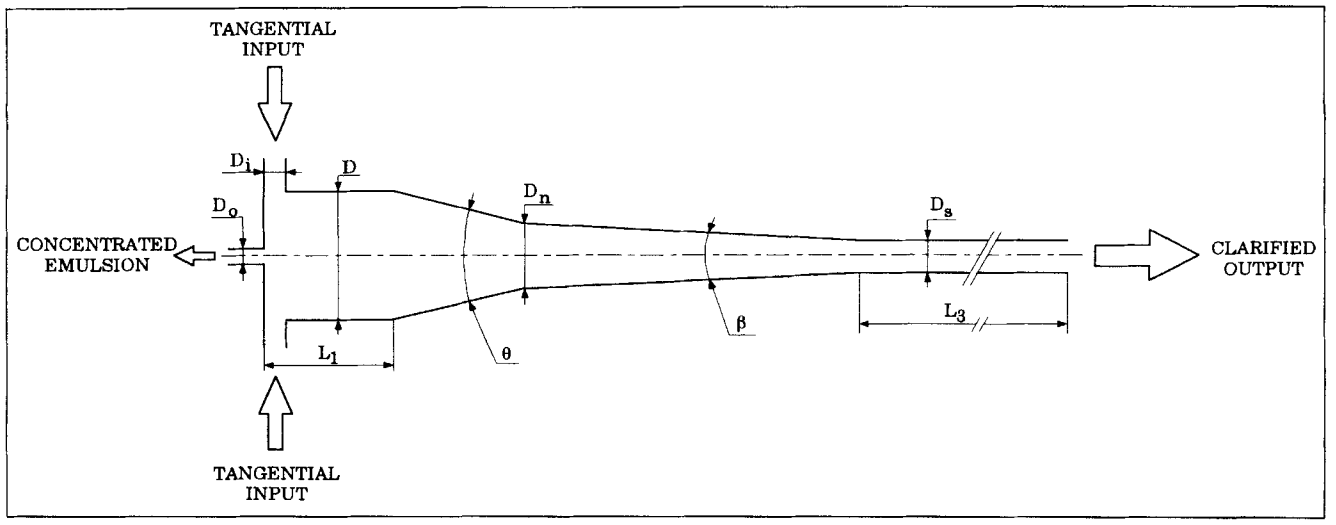

Figure 1. Colman and Thew's hydrocyclone design.

$D_n/D = 0.5$; $D_s/D = 0.25$; $D_i/D = 0.175$; $D_o/D < 0.05$; $L_1/D = 1$; $L_3/D = 15$; $\theta = 20°$; $\beta = 1.5°$.

(1988) based on the small specific gravity difference of liquid–liquid emulsions and the function of the hydrocyclone as a clarifier. In order to increase the residence time, a low cone angle section and a cylindrical section have been added (Figure 1). The other major difference is that the continuous phase leaves the apparatus through the underflow outlet and the concentrated oil emulsion leaves through a small overflow outlet. In this article, we consider the second type of hydrocyclone. This version is used in most industrial applications.

A limitation on the use of such devices is the lack of a good procedure for the efficiency calculation of liquid–liquid hydrocyclones that could be used for simulation and design. To overcome this limitation we have developed such a procedure. It is described in the following sections. We first present the equations governing the velocity distributions in a hydrocyclone. Then, after a short presentation of currently used efficiency theories, we develop a trajectory-analysis-based approach to efficiency computation. Following a description of the implementation and of the test example, the results are discussed and conclusions drawn about this new procedure.

Velocity Distributions

The fluid velocity field in a hydrocyclone has three components: the tangential velocity V, the axial velocity W, and the radial velocity U.

Experimental measurements lead to the conclusion that two types of vortices occur: a forced vortex for the core and a semifree vortex. The determining separation process takes place in the semifree vortex region where the tangential velocity is usually defined by a modified Helmholz law:

$$V \cdot r^n = C, \tag{1}$$

where n can take a value between -1 (forced vortex) and 1 (free vortex), observed values of n often being in the range of 0.5 to 0.9. The constant, C, can be obtained from the inlet velocity. For a perfectly tangential feed, the tangential velocity near the wall would be equal to the inlet velocity. Equation 1 can thus be rewritten, with the nominal diameter $D_n = 0.5$ D (see Figure 1 for the geometrical proportions):

$$V \cdot r^n = \alpha \cdot \tilde{V}_i \cdot \left(\frac{D}{2}\right)^n = \alpha \cdot \tilde{V}_i \cdot D_n^n. \tag{2}$$

The lack of perfection is represented through the coefficient α, which is related to the ratio D_i/D. The inlet diameter, D_i, equals 0.175 D; thus we have $D_i = 0.35 D_n$. The mean feed velocity for two symmetrical inlets is obtained by

$$\tilde{V}_i = \frac{4 \cdot (Q/2)}{\pi \cdot D_i^2} = \frac{4 \cdot (Q/2)}{\pi \cdot D_n^2 \cdot 0.35^2}. \tag{3}$$

Dabir (1983) showed experimentally that Eq. 2 could be used throughout the hydrocyclone, the conical shape inducing an acceleration of the tangential velocity that roughly compensates the loss by friction.

The axial velocity in a Thew-type hydrocyclone shows a two-cell pattern (Colman, 1981). Colman's measurements of the axial velocity for the low cone angle section can be represented through a dimensionless correlation (Ma, 1993):

$$\frac{W}{W_z} = -3.33 + 12.0 \cdot \frac{r}{R_z} - 8.63 \cdot \left(\frac{r}{R_z}\right)^2 + 1.19 \cdot \left(\frac{r}{R_z}\right)^3, \tag{4}$$

where W_z is the mean axial velocity at level z if there is no concentrated emulsion output. It is defined by

$$W_z = \frac{Q}{\pi \cdot R_z^2},$$

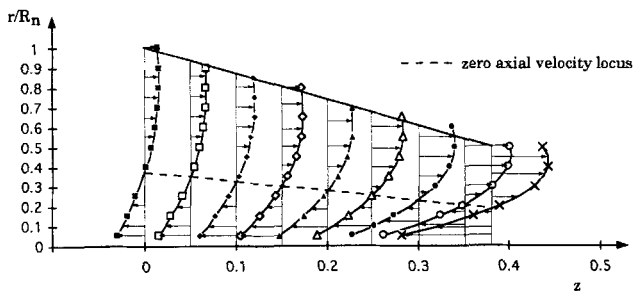

Figure 2. Axial velocity distribution.

where R_z is the radius of the wall at level z and is given by

$$R_z = \frac{D_n}{2} - z \cdot \tan\left(\frac{\beta}{2}\right)$$

with β the angle of the low cone angle section. Figure 2 shows the axial velocity distribution for the low cone angle section using r/R_n, the relative radial position with $R_n = D_n/2$. The locus of zero axial velocity can be deduced from equation (4). The radius of the locus is found to be

$$R_1 = 0.3718 R_z.$$

The radial velocity can be obtained using the continuity equation and the wall condition suggested by Kelsall (1952). This leads to

$$U = -\frac{r}{R_z} \cdot W \cdot \tan\left(\frac{\beta}{2}\right). \tag{5}$$

This is obviously only an approximation since it would mean that only the dispersed phase crossed the locus of zero axial velocity. For Thew-type hydrocyclones, however, the fraction of continuous phase crossing the locus represents only about 1 or 2%, whereas in the more classic Rietema type of hydrocyclone only 1 or 2% of the continuous phase does not cross the locus of zero axial velocity. Equation 5 could be corrected by introducing a mean crossing velocity defined as the flow of concentrated emulsion per unit of locus area.

For the dispersed phase, the droplet settling velocity is usually given by Stokes' law, provided the droplet Reynolds number remains lower than 1, which is usually the case in liquid–liquid hydrocyclones. Replacing the gravitational acceleration by the centrifugal acceleration, the expression of Stokes' law becomes

$$U_d = \frac{\Delta\rho \cdot d^2 \cdot (V^2/r)}{18 \cdot \eta}. \tag{6}$$

Efficiency Theories

The separation in a hydrocyclone is based, on the one hand, on the effect of the centrifugal force induced by the fluid flow, and on the other hand, on the difference in specific gravity between the dispersed and the continuous phases. Since the separation efficiency varies with the particle diameter, instead of estimating a global efficiency, one is led to define a characteristic particle diameter for the given operating conditions. For solid–liquid hydrocyclones, two theoretical approaches emerged during the 60s: the equilibrium locus theory and the residence time theory.

The equilibrium locus theory, best described by Bradley (1965), is based on the fact that, for solid–liquid separation, the solid usually has a higher specific gravity than the liquid. Therefore the radial fluid velocity and the settling velocity are of opposite sign. By equating the settling velocity and the mean radial fluid velocity, a characteristic diameter is obtained. Since particles of that diameter have an equal probability of leaving the hydrocyclone within the bulk phase or within the concentrated output, the diameter is expressed as d_{50}. Obviously, this theory cannot be applied when the dispersed phase has a lower specific gravity than the continuous phase, which is often the case in liquid–liquid separations. Since both velocities have the same sign, no equilibrium locus exists.

The second theory, developed by Rietema (1969), uses the decantation theory based on the residence time of a particle in the hydrocyclone. He argues that, if a particle of a given diameter, entering the hydrocyclone in the center of the inlet pipe, reaches the wall exactly at the beginning of the outlet pipe, then, assuming a homogeneous distribution over the inlet section, particles of that diameter have a 50% probability of being separated. Therefore a characteristic diameter d_{50} can be defined. However, a constant ratio U/W is assumed. This is only valid if the inlet diameter is small compared to the hydrocyclone's nominal diameter and if the particle remains close to the wall. The latter condition is, however, not verified for liquid–liquid separations where the droplets are collected in the core of the hydrocyclone.

Both theories, while well-suited to solid–liquid separations, appear to be less attractive for liquid–liquid separations in a Thew-type hydrocyclone. Therefore, in the next section we present a new approach that is also based on the decantation theory.

Efficiency through Trajectory Analysis

From a theoretical point of view, a hydrocyclone is similar to a decanter where the gravitational force has been replaced by a centrifugal force. The only difference is that the velocities, constant in a decanter, have a spatial dependence in a hydrocyclone. This will increase the computational effort, but has no effect on the theoretical development.

The trajectory of a droplet can be characterized through a relation between the axial and radial coordinates of its position (Ma, 1993). It can be expressed as an ordinary differential equation combining the axial, radial, and settling velocities:

$$\frac{dz}{dr} = \frac{(dz/dt)}{(dr/dt)} = \frac{W}{U + U_d}. \tag{7}$$

Let us denote the third-order polynomial correlation of Eq. 4 by P_3. Replacing the velocities in Eq. 7 by their expressions (Eqs. 2 to 6), we get

$$\frac{dz}{dr} = \frac{\left(P_3 \cdot \frac{Q}{\pi \cdot R_z^2}\right)}{\left[\frac{2}{9 \cdot \pi^2} \cdot \frac{\alpha^2}{0.35^4} \cdot \frac{(\rho_d - \rho_c) \cdot d^2 \cdot Q^2}{\eta} \cdot \frac{D_n^{2n-4}}{r^{2n+1}}\right] - \left[\frac{r}{R_z} \cdot P_3 \cdot \frac{Q}{\pi \cdot R_z^2} \cdot \tan\left(\frac{\beta}{2}\right)\right]}.$$

After some manipulations, the equation becomes

$$\frac{dz}{dr} = \frac{\left(\frac{P_3}{R_z^2}\right)}{\left[-St \cdot \frac{\alpha^2}{0.35^4} \cdot \frac{D_n^{2n-1}}{r^{2n+1}}\right] - \left[\frac{r}{R_z} \cdot \frac{P_3}{R_z^2} \cdot \tan\left(\frac{\beta}{2}\right)\right]} \quad (8)$$

where St is the Stokes number

$$St = \frac{2 \cdot \Delta\rho \cdot Q \cdot d^2}{9 \cdot \pi \cdot \eta \cdot D_n^3}.$$

It appears that the Stokes number is the only term in Eq. 8 that relates to the operating conditions of the hydrocyclone: flow, viscosity, specific gravities, and droplet diameter. All the other terms are solely functions of the hydrocyclone's geometrical properties.

Rather than defining the efficiency of a hydrocyclone through the d_{50} diameter as in the theories presented in the preceding section, we prefer to keep the classifying approach used in decantation theory. The characteristic diameter d_{100} corresponds to the smallest droplet diameter with a 100% separation efficiency. This allows us to compare the efficiencies of hydrocyclones with those of a classic decanter. The comparison of the d_{50} diameter would, on the other hand, require that both apparatuses have identical efficiency distributions.

The d_{100} diameter can be found by considering a droplet entering the hydrocyclone at the wall and reaching the locus of zero axial velocity just before the bulk flow leaves the apparatus. If this droplet reaches the locus, then its radial velocity (settling velocity) will make it cross the locus and it will be carried out within the concentrated output. The critical trajectory will be

$$\int_{r=(D_n/2)}^{r=R_L} \left(\frac{dz}{dr}\right) \cdot dr = L, \quad (9)$$

with L the length of the hydrocyclone and R_L the radius of the locus of zero axial velocity at L:

$$R_L = 0.3718 \cdot \left[\frac{D_n}{2} - L \cdot \tan\left(\frac{\beta}{2}\right)\right].$$

For a given geometry, Eq. 9 can be regarded as a nonlinear equation of the Stokes number. The solution of that equation leads to the value of St_{100}, which is unique for a given hydrocyclone. The d_{100} diameter, depending on the operating conditions and the fluid properties, can then be deduced:

$$d_{100} = \sqrt{\frac{9 \cdot \pi \cdot \eta \cdot D_n^3}{2 \cdot \Delta\rho \cdot Q} \cdot St_{100}}. \quad (10)$$

An interesting property of this formulation is that solving Eq. 9 only once for a given hydrocyclone allows the d_{100} diameter to be determined for a whole range of emulsions and flow rates.

The efficiency distribution can also be obtained. If a droplet of diameter d having the initial position at radius R_d has a trajectory verifying the following equation

$$\int_{r=R_d}^{r=R_L} \left(\frac{dz}{dr}\right) \cdot dr = L, \quad (11)$$

then any droplet of that diameter introduced at a radius greater than R_d will not be separated, while the same droplet introduced at a smaller diameter will be separated. The efficiency for a droplet diameter can therefore be expressed by the ratio of the efficient inlet area over the total inlet area, assuming a homogeneous distribution over the total inlet area. If we consider that only the low cone angle section has a real separative power, then the total inlet area is located between the locus of zero axial velocity and the wall. The efficiency becomes

$$E(d) = \left[\frac{\pi \cdot R_d^2 - \pi \cdot (0.3718 \cdot R_n)^2}{\pi \cdot R_n^2 - \pi \cdot (0.3718 \cdot R_n)^2}\right]. \quad (12)$$

Global efficiency can then be obtained for a given emulsion, provided the droplet distribution is known. Usually a discrete form of the following equation is used:

$$EFF = \int_{\phi=0}^{\phi=d_{100}} E(\phi) \cdot p(\phi) \cdot d\phi + \int_{\phi=d_{100}}^{\phi=\infty} p(\phi) \cdot d\phi, \quad (13)$$

where $p(d)$ is the probability density function of the droplet distribution.

Thus far, we have just considered the low cone angle section, but the cylindrical section also has a separating effect. However, no velocity measurements are available. To study this section, we therefore had to make some assumptions:

- The axial velocity profile at the end of the conical section is maintained throughout the cylindrical section.
- The remaining radial fluid velocity can be neglected.
- For the tangential velocity, we considered two cases: (1) there are no friction losses; (2) the tangential velocity decreases linearly, and the velocity at the end of the cylinder represents only 30% of the initial velocity.

The two assumptions on the tangential velocity in the

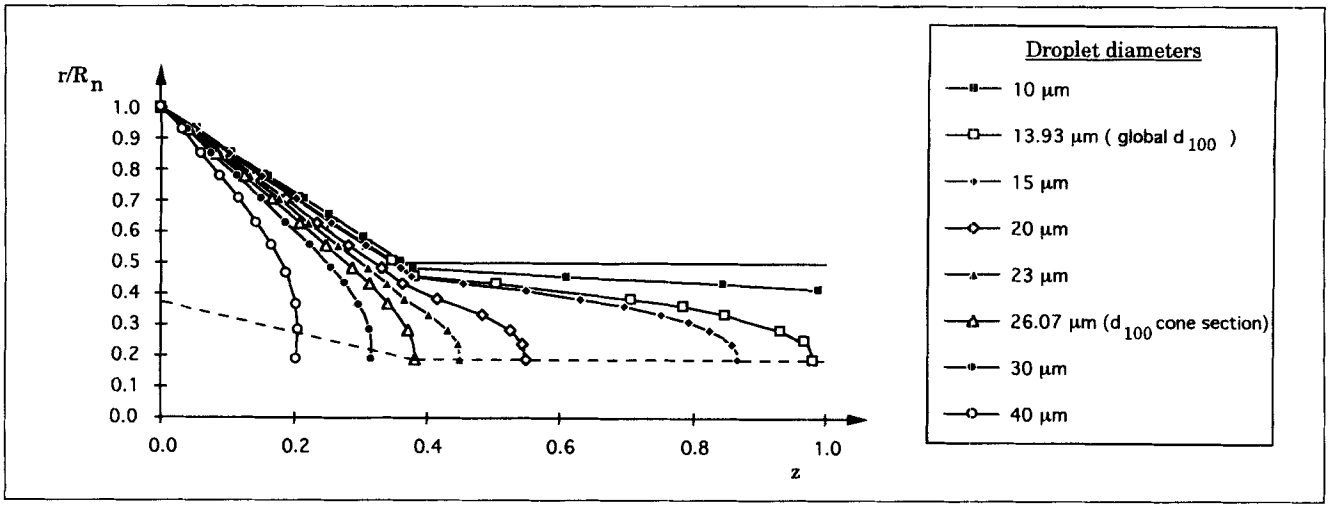

Figure 3. Maximal trajectories and d_{100} determination with constant tangential velocity in the cylindrical section.

cylindrical section have been set up on an academic basis, because no experimental data are available for the velocity profiles in this section. The first assumption leads clearly to a rough overestimation of the efficiency of the hydrocyclone. The second assumption is based on some of the results and assumptions of Hargreaves and Silvester (1990) for their numerical simulation of the flow pattern in a Thew-type hydrocyclone:

- There exists some residual swirl at the end of the cylindrical section;
- The rate of angular momentum decay is considered to be locally constant and friction driven;
- Their first simulation results presented an approximate 2 to 2.5% decay per dimensionless unit of L_3/D_n during the first half of the cylinder, where the exit boundary conditions have lesser effect.

For our hydrocyclone, L_3/D_n equals 30; thus an average of 70% decay of the tangential velocity in this section could be a realistic option.

Implementation and Test Example

The approach just described has been implemented on a VAX computer using the FORTRAN language. A program called CYCLO offers two options:

1. Integration of the ordinary differential equation (Eq. 8) using a fourth-order Runge-Kutta method.
2. Resolution of the critical trajectory equations (Eq. 9 or 11) according to the initial position of the droplet. The procedure solves Eq. 8 iteratively in order to determine the droplet diameter for which Eq. 9 or 11 is satisfied.

Given the droplet distribution of an emulsion and the efficiency distribution of an apparatus (not necessarily a hydrocyclone), a second program, EFFI, computes the total yield, the yield per size class, and the residual droplet distributions and concentrated fluid droplet distributions using Eq. 13.

The test example conditions were selected among the sets of experiments carried out by Ma (1993) at the Elf Aquitaine research center in Boussens. The hydrocyclone had a nominal diameter D_n of 0.02 m, the low cone angle section had an angle of 1.5°, while the angle of the upper section was 20°. The geometrical ratios given for the Thew-type hydrocyclone in Figure 1 were respected. For the tangential velocity formula 2, the best fit to Colman's measurements (1981) was obtained with $\alpha = 0.5$ and $n = 0.65$.

The reference emulsion was an oil/water emulsion from the oil fields of southwestern France. The difference in specific gravity between water and oil was 98 kg/m^3, with an average emulsion viscosity of 0.001 Ns/m^2. A flow rate of 1.943 m^3/h of emulsion, with a concentration of 0.5 g oil/L, was treated by the hydrocyclone. The experimentation was carried out at room temperature.

The droplet size distributions (Figure 7) have been obtained using the CILAS ALCATEL 715 granulometer. The major advantage of this laser technique is the short response time (about 1 min), thus avoiding excessive coalescence and sedimentation during the analysis.

Results and Discussion

First we examine the trajectories of droplets of different sizes within the hydrocyclone, with and without decreasing tangential velocity in the cylindrical section, plotted using a projection on a half-axial cutting plane (Figures 3 and 4). The trajectories of the d_{100} droplet for the low cone angle section and for the whole hydrocyclone have also been plotted.

The d_{100} value of the low cone angle section is 26 μm. The d_{100} for the whole hydrocyclone is 14 μm when a constant tangential velocity is considered for the cylindrical section, and 17.7 μm if the tangential velocity loses 70% of its initial value in that section. The relevance of such a section, which Thew added specially for liquid–liquid separations, is confirmed. Through an important increase in the residence time, the droplet is subjected to the centrifugal force much longer. The efficiency is thereby almost doubled even if the tangential velocity decreases significantly.

It clearly appears that the most effective separation takes place during the last third of the droplet's path. Its settling velocity increases (more than quadratically) fortyfold along the path leading to the oil core.

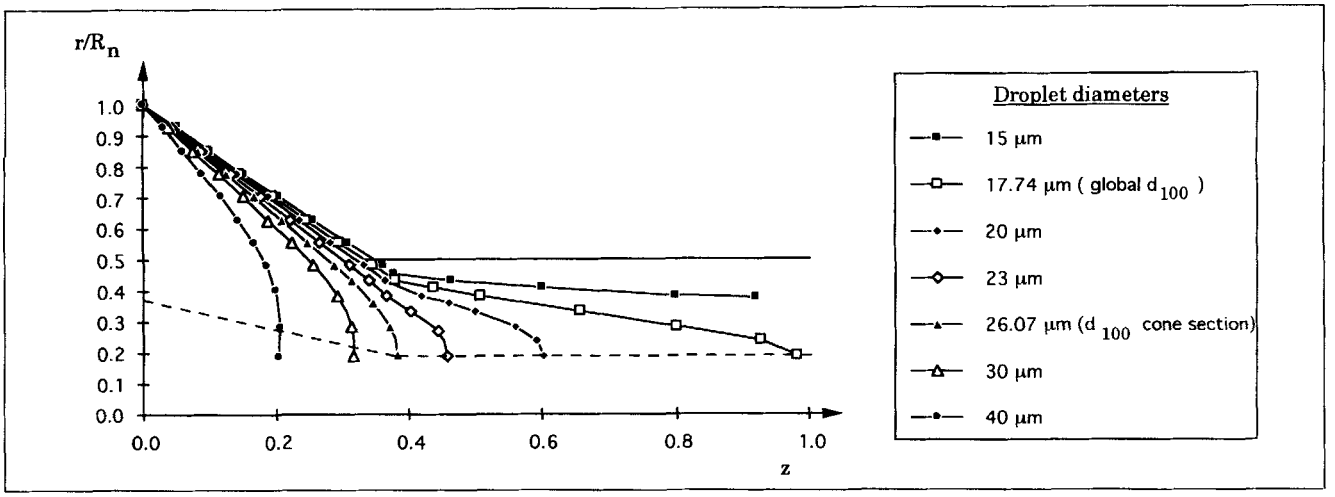

Figure 4. Maximal trajectories and d_{100} determination with decreasing tangential velocity in the cylindrical section.

Another interesting aspect of the cylindrical section is its capacity as classifier. In Figure 4, we note that the cylinder needs to be about 0.4 m longer to totally separate 17.7 μm droplets than it does for the total elimination of 20 μm droplets. Unlike the conical sections, the length of the cylinder can quite easily be modified, thus modifying the global d_{100} value.

Figure 5 shows some critical trajectories for the efficiency distribution determination in the case of decreasing tangential velocity. The efficiency distributions are obtained by combining these results, as well as those for the low cone angle section and the constant tangential velocity case, with the results of Eq. 12. Experimental measurements have been made by Ma (1993) for the whole hydrocyclone and for a hydrocyclone with the cylindrical section removed. For this second case, the axial velocity distribution had to be slightly modified in order to generate an apex of the locus of zero axial velocity at the end of the low cone angle section. The forced vortex model of the tangential velocity had to be introduced as well for the behavior near the axis. Figure 6 shows the different theoretical and experimental efficiency distributions obtained.

As expected, the efficiency distributions closest to the experimental distributions are obtained with the most realistic models: whole hydrocyclone—model with a decrease in the tangential velocity in the cylindrical section; hydrocyclone without a cylindrical section—model with a modified axial velocity profile.

The theoretical and experimental results coincide quite well if one takes into account the fact that velocity profiles and separation experiments were not carried out under the same conditions in all of the hydrocyclones. On average, the theoretical efficiencies for the given diameters are 15 to 20% higher than the observed values.

The predictions of the d_{100} value are not as good. Three phenomena may explain this discrepancy:

- The flow in the hydrocyclone is turbulent. The droplets are subjected to turbulent diffusion that randomly affects

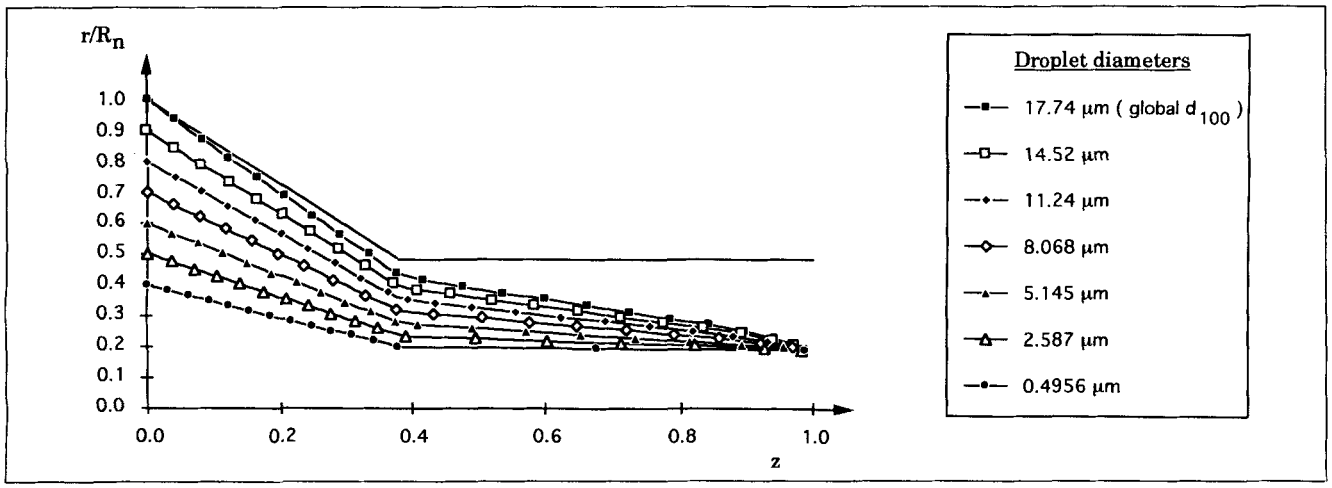

Figure 5. Critical trajectories for efficiency computation with decreasing tangential velocity in the cylindrical section.

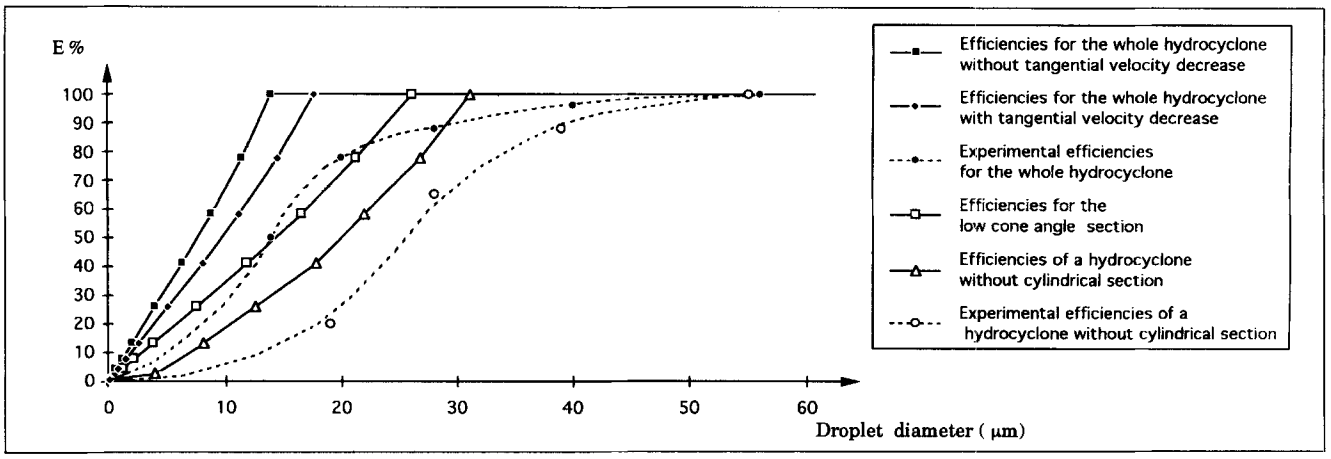

Figure 6. Theoretical and experimental efficiency distributions.

their true trajectories. The velocity distributions and therefore the trajectories are only mean approximations. One can assume that only about 50% of the droplets with diameter d_{100} that should follow the critical trajectory are effectively separated.

- Droplet collision can also lead to a broader efficiency distribution: large droplets are slowed down through collision with small droplets, while small droplets are pushed or dragged along by larger ones.
- A coalescence phenomenon could occur within the hydrocyclone or during the sampling and analyzing process of the emulsions. As a matter of fact, excessively high efficiencies, up to 60%, have sometimes been observed for very small droplets (less than 3 μm in diameter). The hydrocyclone, however, could only account for a few percent, clearly indicating an additional consumption process.

Finally, an example of residual droplet distribution and cumulated mass fraction is presented in Figure 7, using the theoretical efficiency distribution for a hydrocyclone with a decrease in the tangential velocity in the cylindrical section. An overall mass efficiency of 90% was estimated for this example, while the experimental overall efficiency was found to be

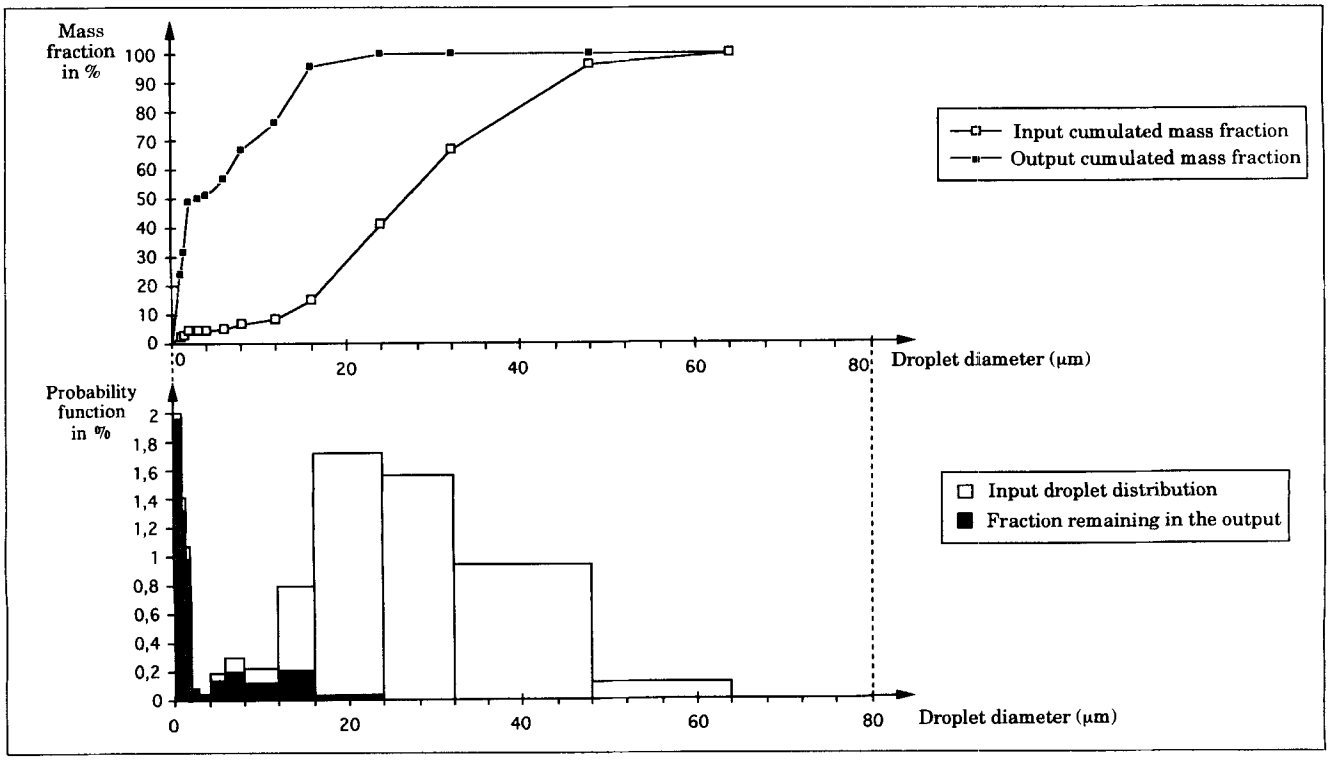

Figure 7. Example of residual droplet distribution for a hydrocyclone with decreasing tangential velocity in the cylindrical section.

81%. This difference is, of course, related to the gap between theoretical and experimental efficiency distributions observed in Figure 6.

A question that remains partially open is: To what extent can the experimentally tuned parameters (α, n, coefficients of P_3) be used for other geometrical proportions than the ones given in Figure 1? Unfortunately, the available velocity measurements within a Thew-type hydrocyclone (Colman, 1981; Hargreaves and Silvester, 1990) have been carried out using laser Doppler anemometry on hydrocyclones that have the same geometrical proportions. Lilge (1962) pointed out that α follows a power law of the ratio D_i/D. The parameter n and the coefficients of P_3 do not represent the intensity, but the relative radial variations, that is, the shape, of a velocity profile. It seems therefore not unrealistic to expect that these parameters depend mainly upon the flow conditions, for example, the overflow to underflow ratio, and the properties of the fluid, for example, the viscosity. Since most current applications of this type of hydrocyclone concern oil-in-water emulsions, and the overflow-to-underflow ratios used rarely exceed the 1 to 2% range, the values for n and the P_3 coefficients suggested by Ma (1993) might still be used for slightly modified geometries.

Conclusions

The theoretical approach to efficiency estimation of liquid–liquid hydrocyclones developed in this article for the Colman and Thew (1988) type of hydrocyclone thus far appears to be an efficient method for making a quick but rough estimation of the efficiency distribution. And this despite the fact that fewer assumptions have been made than in the classic efficiency theories available for solid–liquid hydrocyclones. These results clearly indicate that, for the case of liquid–liquid dispersions with a dispersed phase lighter than the continuous phase, other parameters have to be taken into account.

Two phenomena, specific to liquid–liquid dispersions, should certainly be introduced into the model: coalescence and the breakup of droplets. Because of the small density difference, a strong centrifugal force has to be created within an apparatus of relatively small volume, thus creating the large velocity gradients leading to shear stresses strong enough to break up some of the droplets. On the other hand, but for the same reason, the residence time and the trajectory length are much greater than for solid–liquid dispersions. This increases the collision probability of the droplets, which is the first step to coalescence.

Turbulent diffusion may also have a greater influence than for solid–liquid dispersions: the inertia of a given droplet is much smaller than for a particle of the same size, again due to the small density difference. Hence a droplet should be more sensitive to the random turbulent motion of the surrounding fluid.

However, taking some or all of these features into account when formulating the model would drastically increase its complexity and its computation time (so far the program requires only a few seconds to determine a d_{100} value). Setting up a model based on the foregoing concepts could be the aim of future studies. These would seek a better compromise between (1) accuracy and reliability, and (2) complexity, time requirements, and data requirements.

Notation

D = diameter of the hydrocyclone at the inlet level (m)
E = efficiency distribution
p = droplet size distribution or mass distribution
Q = flow rate (m^3/s)
r = radial coordinate (m)
U_d = settling velocity (m/s)
$\bar{V}_i$ = mean feed velocity (m/s)
z = axial coordinate (m)

Greek letters

α = fraction of inlet velocity contributing to the initial tangential velocity
ρ = specific gravity (kg/m^3)
η = viscosity (Ns/m^2)

Literature Cited

Bradley, D., *The Hydrocyclone*, Pergamon, London, p. 330 (1965).

Dabir, B., "Mean Velocity Measurements in a 3″-Hydrocyclone Using Laser Doppler Anemometry," PhD Thesis, Michigan State Univ., East Lansing (1983).

Colman, D. A., "The Hydrocyclone for Separating Light Dispersion," PhD Thesis, Dept. of Mechanical Engineering, Southampton Univ., Southampton, England (1981).

Colman, D. A., and M. T. Thew, "Cyclone Separator," U.S. Patent 4764287 (Aug. 16, 1988).

Hargreaves, J. H., and R. S. Silvester, "Computational Fluid Dynamics Applied to the Analysis of Deoiling Hydrocyclone Performance," *Trans. Ind. Chem. Eng., part A*, **68**, 365 (July, 1990).

Kelsall, D. F., "A Study of the Motion of Solid Particles in a Hydraulic Cyclone," *Trans. Inst. Chem. Eng.*, **30**, 87 (1952).

Lilge, E. O., "Hydrocyclone Fundamentals," *Trans. Inst. Min. Metall.*, **71**, 295 (1962).

Ma, B.-F., "Epuration des eaux résiduaires de l'industrie pétrolière par hydrocyclonage," PhD Thesis, Institut National des Sciences Appliquées de Toulouse, Toulouse, France (1993).

Rietema, K., "Performance and Design of Hydrocyclones: I, II and III," *Chem. Eng. Sci.*, **15**, 298 (1969).

Manuscript received Dec. 30, 1993, and revision received Aug. 4, 1994.